Molecular Motion in Solid Tetramethylammonium Tetrafluoroborate

S. Torre

Dipartimento di Fisica "A. Volta", Università di Pavia, Via Bassi 6, I-27100 Pavia, Italy

P. Ferloni

Dipartimento di Chimica Fisica della Università and CSTE-CNR, viale Taramelli 16, I-27100 Pavia, Italy

Z. Naturforsch. **47a**, 721–727 (1992); received March 24, 1992

Measurements of ^{11}B and ^{1}H NMR relaxation times, differential scanning calorimetry and thermomechanical analysis, carried out on polycrystalline $(CH_3)_4NBF_4$ from room temperature to about 100 K, have permitted to discuss the crystal dynamics of this salt and to analyze the nature of the phase transition occurring at $\approx$150 K. Moreover, by means of an evaluation of the ^{11}B quadrupole coupling constant, information about the position of the F atoms has been obtained. An explanation of the NMR data in terms of an order-disorder phase transition involving the F^- ions is given.

Key words: $(CH_3)_4NBF_4$, Molecular motion, Phase transition.

Introduction

Among the supporting electrolytes most commonly used in electrochemistry, several tetraalkylammonium salts, both symmetrical and asymmetrical, have been characterized and widely applied in aqueous and non-aqueous systems. The tetrafluoroborates, in particular, have been studied mainly from the standpoint of their behaviour in solution or in the molten state, whereas poor information is available on their properties in the solid state.

In a previous paper [1], the thermal behaviour of four symmetrically substituted ammonium tetrafluoroborates, from tetramethyl- to tetra-n-butyl-, was reported. As for $(CH_3)_4NBF_4$, NMR preliminary data were presented [2, 3] and the crystal structure at room temperature was determined by means of X-ray diffraction on single crystal [4].

A distinctive feature of this structure is the association in the 4/mmm Laue symmetry, P4/nmm space group, of the tetrafluoroborate anion, which is "disordered", with the substituted ammonium cation, which is "ordered". The boron atom and one of the fluorine atoms, F_a, lie on the tetragonal axis of the elementary cell, whereas the remaining three F atoms, F_b, can rotate around it and are therefore related to a trigonal axis, as shown in Figure 1. The coincidence of the latter axis with the tetragonal one, i.e. of two incompatible axes, allows the BF_4 tetrahedra to occupy either a general or a special *m* point symmetry, with a remarkable positional disorder [4].

In the light of these observations it seemed worthy to study the crystal dynamics of $(CH_3)_4NBF_4$ at room and low temperatures. In the present paper, the results of measurements carried out by means of nuclear magnetic resonance and thermal techniques are reported. The existence of the phase transition previously detected [1] at about 150 K has been confirmed, and the nature of the molecular motions in the solid phases is briefly discussed.

Experimental

The $(CH_3)_4NBF_4$ powder products supplied by Aldrich and Fluka were dried in vacuo at 100 °C before use and did not show any significant difference in their thermal behaviour. Pellets about 1 mm high and 4 mm in diameter, pressed at 10^3 kg cm^{-2}, were also prepared with the Aldrich salt for thermomechanical analysis (TMA). Differential scanning calorimetry (DSC) was performed with a Perkin-Elmer Mod. DSC-2 instrument as previously reported [1], with He as purge gas; TMA scans were carried out with a Du Pont mod. 943 Thermomechanical Analyzer, driven

Reprint requests to Prof. Paolo Ferloni, Dipartimento di Chimica Fisica, Viale Taramelli 16, I-27100 Pavia, Italy.

0932-0784 / 92 / 0600-0721 $ 01.30/0. – Please order a reprint rather than making your own copy.

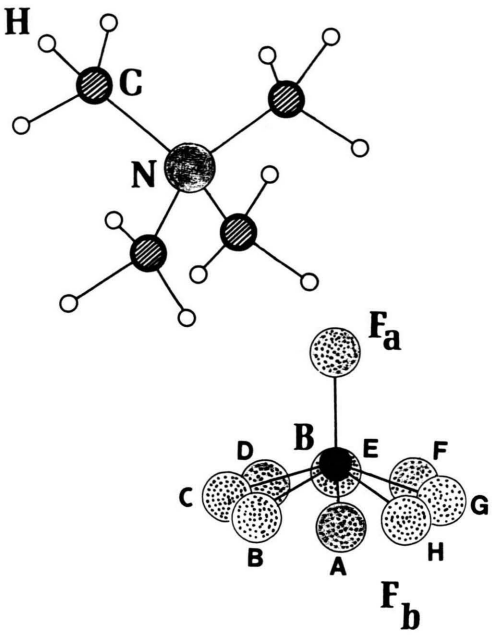

Fig. 1. Crystal structure of $(CH_3)_4NBF_4$ (one half of the cell is shown).

by a Thermal Analyst 2000 unit, with a heating rate of 5 K min^{-1} in nitrogen flow.

The NMR measurements were carried out on powdered samples by using a Fourier transform (FT) pulse spectrometer operating at variable frequency (5–60 MHz) in connection with an electromagnet.

The ^1H spin-lattice relaxation time T_1 was measured as a function of temperature between room temperature (RT) and about 120 K at a Larmor frequency $\nu_L = 20$ MHz. In the study of the recovery law a saturating sequence of about ten $\pi/2$ pulses has been used to induce complete equalization in the populations of the Zeeman levels. Then, the growth of the magnetization was monitored from the free induction decay (FID) signal $s(t)$ a time t later. The spectra were taken as FT of the free precession signal or of the echo signal.

The amplitude of the radiofrequency field H_1 was around 45 G, and the static magnetic field H_0 about 4700 G. In the same temperature range, ^{11}B T_1 measurements were performed at different Larmor frequencies. The ^{11}B NMR central line is broadened by second-order quadrupole effects in a frequency range $\approx 0.5\, \nu_Q^2/\nu_L$, where ν_Q is the quadrupole coupling constant. In order to obtain a reliable evaluation of ν_Q, the dephasing time τ_Q of the FID of the central line $(-1/2 \leftrightarrow +1/2)$ was measured as a function of ν_L as explained in the following section.

The recovery of the z-component of the nuclear magnetization ($z \parallel H_0$) was monitored after a short saturating pulse sequence that is believed to saturate the central line without affecting the remaining levels. The recovery law was almost exponential in the whole temperature range even though in some instances a slight non-exponential decay was observed. The temperature stabilization was always within 0.1 K.

Results and Discussion

Thermal Measurements

In order to confirm the existence of the phase transition previously detected around 154 K [1], further DSC scans were carried out by heating at different scan speeds, both lower and higher than that (10 K min^{-1}) currently employed in DSC work in this laboratory. It is well known that one can enhance the sensitivity of the DSC technique by increasing the scan speed, thus detecting peaks associated with sluggish thermal phenomena, which usually look as smooth humps in the energy vs. temperature plot. On the other side, small peaks can be singled out by choosing a low scan speed with a high sensitivity. However, a drawback of this choice at low temperatures, besides the increased noise, is the higher curvature of the base line, overlapping with the natural curvature of the C_p's as a function of temperature in this T range. Thus, the interpretation of the obtained plots can be relatively difficult. The present DSC results prove that this transition, although associated with a very small latent heat, occurs reversibly. The peak area and the temperature range are practically independent of the scan rate both on cooling and on heating.

In Fig. 2, DSC traces recorded on cooling and heating are illustrated. The solid-to-solid transformation looks like a smooth phase transition, beginning at about 140 K and displaying the peak maximum at ≈ 160 K. Due to the difficulty in tracing the base line, the peak area could only roughly be evaluated, giving a transition enthalpy of 0.5 ± 0.1 kJ mol^{-1}.

An example of a TMA trace in the same temperature range is shown in Figure 3. The phase transition is displayed in this plot as a small decrease in volume on heating the sample at ≈ 140 K, followed by a regular increase at higher temperatures. This uncommon

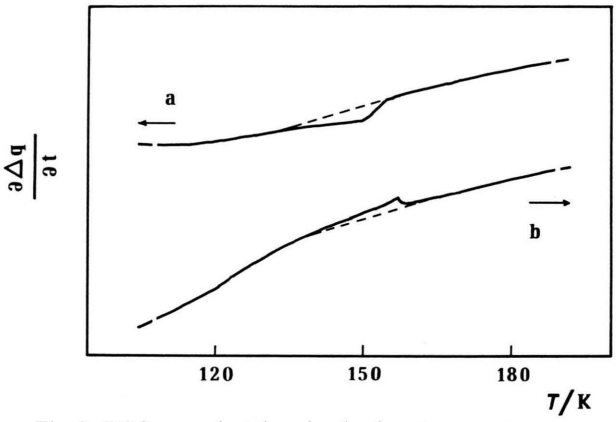

Fig. 2. DSC records taken in the low temperature range: a) on cooling, scan speed 40 K min^{-1}; b) on heating, scan speed 10 K min^{-1}.

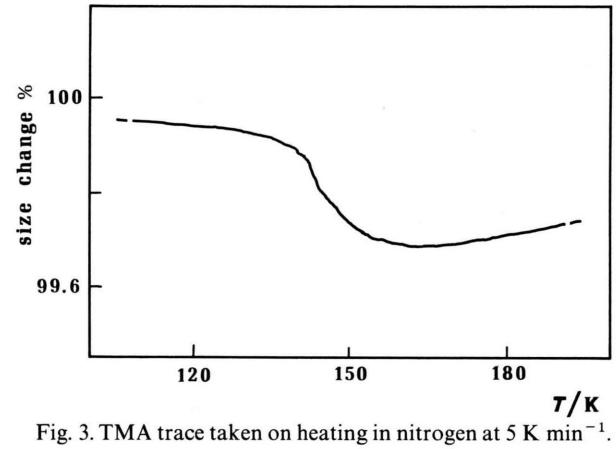

Fig. 3. TMA trace taken on heating in nitrogen at 5 K min^{-1}.

feature is similar to the volume increase observed on cooling NH_4BF_4 at about 170 K [5], and also to that corresponding to the cubic-tetragonal transition of NH_4Br and NH_4I [6].

^1H NMR and Relaxation

Figure 4 shows the spin-lattice relaxation rate $R = T_1^{-1}$ for protons vs. inverse temperature at Larmor frequencies of 20 and 60 MHz, the latter data having been taken from [2]. On cooling from room temperature, R shows a maximum at 222 K for $\nu_L = 20$ MHz and at about 250 K for $\nu_L = 60$ MHz. A sudden jump to higher values is observed at $T_c = 142$ K, and below this temperature R shows a further increase.

The ^{1}H spin-lattice relaxation rate is driven by the dipole-dipole interaction of the protons with: i) protons belonging to the same CH_3-group (intra-CH_3-dipole-dipole interaction); ii) protons belonging to different groups (inter-CH_3-dipole-dipole interaction); and iii) ^{19}F, ^{11}B nuclei.

As regards the interaction i) we assume, for simplicity, that the CH_3-group is an about equilateral three-spin set with internuclear separation r, reorienting about its threefold axis at random between three equilibrium positions with correlation time τ_{c_1}. The rotation axis is tumbling in three dimensions with correlation time τ_{c_2}.

The spin-lattice relaxation rate produced by intra-CH_3-dipole-dipole interaction can therefore be written [7] as

$$R_{\text{intra}} = T_1^{-1} = \frac{3}{20} \frac{\gamma_H^4 \hbar^2}{r^6} [g(\nu_L, \tau_{c_2}) + 3g(\nu_L, \bar{\tau})], \quad (1)$$

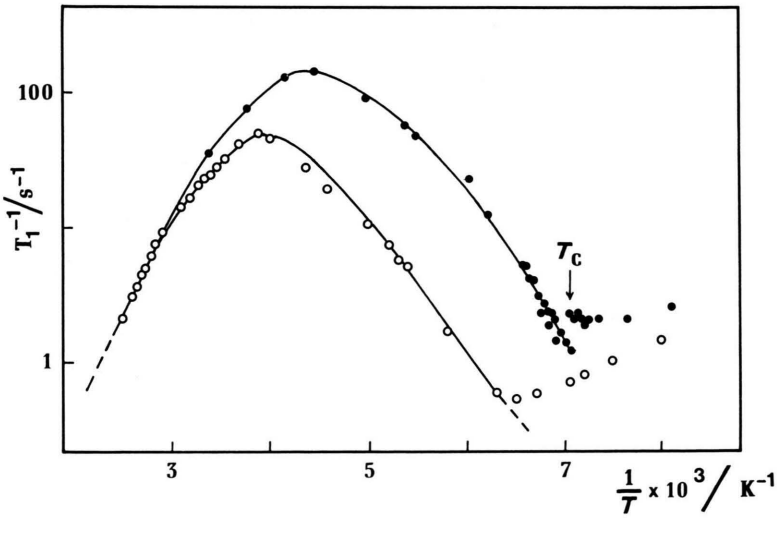

Fig. 4. Temperature dependence of proton spin-lattice relaxation rate, T_1^{-1}, at $\nu_L = 20$ MHz (●) and $\nu_L = 60$ MHz (○). The solid lines are the best fit according to (1) in the text.

where

$$g(\nu_L, \tau) = \frac{\tau}{1+4\pi^2\nu_L^2\tau^2} + \frac{4\tau}{1+16\pi^2\nu_L^2\tau^2}$$

and

$$\bar{\tau}^{-1} = \tau_{c_1}^{-1} + \tau_{c_2}^{-1}\,.$$

The experimental data can be fitted well in the temperature range $300 > T > 142$ K on the basis of (1) by assuming $\tau_{c_1} \gg \tau_{c_2}$ and for τ_{c_2} a thermally activated temperature dependence $\tau_{c_2} = \tau_0 \exp(E_a/kT)$.

The best-fit line with $\tau_0 = 1.8 \times 10^{-14}$ sec and $E_a = 5.6$ kcal mol^{-1} is the solid curve in Figure 4. The maximum for R is predicted at $\nu_L\,\tau_{c_2} \approx 0.1$ with the value $R_{max} = 0.136\,\gamma_H^4\hbar^2/\nu_L r^6$. Assuming $r = 1.7$ Å from X-ray diffraction measurements [4], one obtains for $\nu_L = 20$ MHz, $R_{max} = 165$ sec^{-1} and for $\nu_L = 60$ MHz, $R_{max} = 55$ sec^{-1}, in good agreement with the experimental values 160 and 50 sec^{-1} shown in Figure 4.

Thus it can be concluded that for $T > 142$ K the proton relaxation is driven by intra-CH_3-dipole-dipole interactions, the magnetic interactions between protons belonging to different groups and between protons and ^{11}B and ^{19}F nuclei being almost negligible. This was also suggested by Jurga et al. [2] on the basis of the very similar behaviour of T_1 in $(CH_3)_4NBF_4$ and in the isomorphous $(CH_3)_4NClO_4$.

The fact that, in the crystal structure at room temperature, the distance between every proton and other magnetic moments is almost two times the distances between protons in the same CH_3-group, seems to agree with the above conclusion. It can also be remarked that the best fit gives $\tau_{c_1} \gg \tau_{c_2}$, i.e., the motion of the $(CH_3)_4N^+$ ion as a whole is faster than the rotation of the CH_3-group.

The theoretical rigid-lattice second moment $M_{2H}^{R.L.}$ was also calculated using the Van Vleck formula [8]

$$M_{2H}^{R.L.} = \langle(\nu-\nu_L)^2\rangle$$

$$= \frac{3\,g_H^4\,\beta^4\,I(I+1)}{4h^2} \sum_{K\neq J} \frac{1}{r_{JK}^6}(1-3\gamma_{JK}^2)^2$$

$$+ \frac{g_H^2\,\beta^4}{3h^2} \sum_{K\neq J} S_K(S_K+1)\,\frac{g_K^2}{r_{JK}^6}(1-3\gamma_{JK}^2)^2\,. \quad (2)$$

For a polycrystalline sample, by averaging the direction cosines γ_{JK} over a sphere, one obtains $M_{2H}^{R.L.} = 6.0 \times 10^8$ Hz^2, and for the full width at half intensity, $\delta\nu^{R.L.} = 58$ kHz.

The rigid-lattice $\delta\nu^{R.L.}$ can be compared with the experimental values at 293 K, $\delta\nu = 20$ kHz, and at 150 K, $\delta\nu = 30$ kHz, showing that motional narrowing occurs also at low temperatures. This might be related to methyl group reorientations at frequencies $\tau_{c_1}^{-1} \approx 10^5$ Hz.

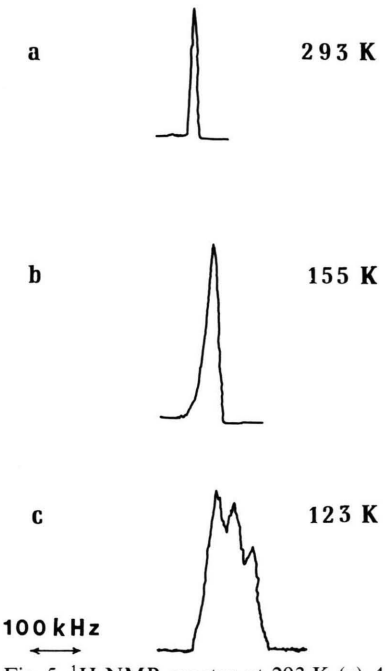

Fig. 5. ^{1}H NMR spectra at 293 K (a), 155 K (b), and 123 K (c) for an external magnetic field $H_0 = 4700$ G.

Below the transition temperature $T_c = 142$ K the ^{1}H NMR line becomes structured, with three well-resolved peaks, and very enlarged, as shown in Figure 5. The sudden jump in the spin-lattice relaxation rate at the transition point might be related to the change in the activation energy of the tumbling motion around the central nitrogen or to a change in the dynamics.

^{11}B NMR and Relaxation

The ^{11}B ($I = 3/2$) NMR spectrum consists of one central line ($m = 1/2 \leftrightarrow -1/2$ transition) and two satellite lines ($\pm 3/2 \leftrightarrow \pm 1/2$) broadened by first-order quadrupole effects in the frequency range $(\nu_L - \nu_Q) \div (\nu_L + \nu_Q)$, where $\nu_Q = \dfrac{e^2 Q q}{h}$ is the quadrupole coupling constant (Q being the ^{11}B nuclear quadrupole moment, $= 3.56 \times 10^{-26}$ cm^2, and $eq = V_{ZZ}$ the largest component of the electric field gradient). The ^{11}B signal was maximized by a pulse length $\tau_{\pi/2}/2$, where $\tau_{\pi/2}$ is

Table 1. Electric field gradient acting at the boron site, for different BF_4 configurations, expressed in $e \times 10^{24}$ units.

Configuration	V_{XX}	V_{YY}	V_{ZZ}
A–C–E	0.21	0.63	−0.84
A–D–F	−0.06	−0.61	0.67

the pulse length maximizing the signal in a H_3BO_3 water solution. Thus, only the central line was irradiated [9]. The second order quadrupole effects broaden this line in a frequency range $\approx 0.5\, \nu_Q^2/\nu_L$.

It can be proved that the free precession signal is approximately gaussian, with a dephasing time τ_Q given by [10]

$$\tau_Q = R_\eta\, \nu_L/\pi\, \nu_Q^2\,,$$

where R_η is a factor slightly depending on the asymmetry parameter $\eta = (V_{XX} - V_{YY})/V_{ZZ}$ ($R_\eta = 3.05$ for $\eta = 0$ and $R_\eta = 2.65$ for $\eta = 1$).

Thus, by measuring ν_Q as a function of ν_L, the value $\nu_Q = 660 \pm 20$ kHz was determined, which can be compared with the theoretical one, obtained by calculating the electrical field gradient (EFG) acting on the ^{11}B nucleus.

The F_b^- ions can occupy three of the eight different positions shown in Figure 1. The EFG has been calculated, in a point charge approximation, for occupancy of sites A–C–E, or equivalently, B–D–F, C–E–G, D–F–H, E–G–A, F–H–B, G–A–C, H–B–D, and for occupancy of sites A–D–F, or equivalently, B–E–G, C–F–H, D–G–A, E–H–B, F–A–C, G–B–D, H–C–E, A–C–F, B–D–G, C–E–H, D–F–A, E–G–B, F–H–C, G–A–D, and H–B–E. Configurations with two nearest-neighbour sites occupied at the same time have been neglected because of steric hindrance (distance of ≈ 1 Å vs. ≈ 1.3 Å of the F^- ionic radius). The electric field gradient values are presented in Table 1. One can find:

$\nu_Q^{calc} = 900$ kHz for configuration A–C–E, and equivalent ones;

$\nu_Q^{calc} = 700$ kHz for configuration A–D–F, and equivalent ones.

Both values agree very well with the experimental datum at room temperature $\nu_Q^{exp} = 660 \pm 20$ kHz, if one considers the approximate nature of this calculation, and the fact that any kind of restricted motion reduces the linewidth relative to its rigid lattice value.

Although not allowing one to identify the preferred configuration, these calculations indicate that both types of sites have very similar EFG components. It follows that one does not expect a change in linewidth with temperature, even in the case of energetically different configurations described by Boltzmann statistics: in fact, the linewidth does not change significantly over the entire 140 – 300 K range.

Relaxation measurements were also performed from RT to 142 K. When only the central line is saturated, the recovery of the nuclear magnetization M is given by

$$\frac{M(\infty) - M(t)}{M(\infty)} = \tfrac{1}{2} \exp(-2\, W_1\, t) + \tfrac{1}{2} \exp(-2\, W_2\, t),$$

where W_1 and W_2 are the probabilities for the transition with $\Delta m = 1$ and 2, respectively. For T_1^{-1}, the slope of the recovery law at the origin, $T_1^{-1} = W_1 + W_2$, was assumed. The recovery in the whole temperature range was almost exponential, indicating that $W_1 \approx W_2$.

The relaxation is chiefly driven by the modulation of the ^{11}B EFG associated with the motion of the F atoms across the different configurations analyzed above. A generic expression for the relaxation rate is

$$\frac{1}{T_1} = \frac{1}{2}\, \frac{e^2 Q^2}{\hbar^2}\, \langle \delta V_{zz}^2 \rangle\, \tau\,,$$

where δV_{zz} stresses the fact that this kind of motion modulates only a fraction of the static quadrupolar interaction, and where the dispersionless process $\nu_L \tau \ll 1$ agrees with the observation that T_1 appears to remain always frequency independent.

The major feature of the ^{11}B relaxation will be discussed qualitatively below; the attention is now focussed upon the small bump at ≈ 250 K shown in the inset of Figure 6. Its magnitude is consistent with that expected from the ^{11}B–^{19}F dipolar interaction, and corresponds rather well to a similar anomaly of the ^{19}F relaxation reported by Jurga et al. [2].

The occurrence of a maximum of the dipole induced relaxation without the simultaneous observation of an enhanced, and much larger, quadrupolar contribution, throws light upon the nature of the dynamics of the BF_4 group. At low temperatures, the dynamics of a fluorine can be described as a back and forth motion between neighbouring sites, e.g. G and H in Figure 1.

Such a motion changes substantially the EFG's, but very little the B–F dipolar interaction. On the other hand, when the BF_4 group performs a hindered rotation, with three fluorines, e.g., initially in A–D–F, which end up in D–F–A, the dipolar interaction changes, whereas the EFG does not, until the initial

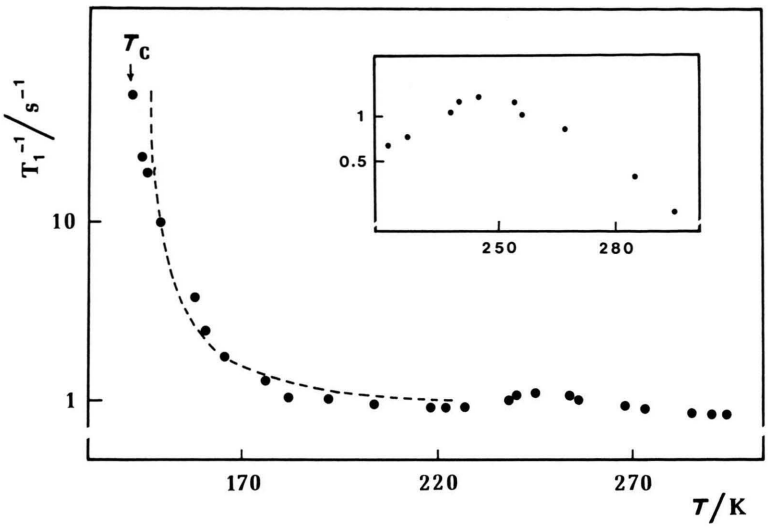

Fig. 6. Temperature dependence of ^{11}B spin-lattice relaxation rate, T_1^{-1}, at $\nu_L = 13.3$ MHz. The dashed line corresponds to the theoretical behaviour according to a $T_1^{-1} \propto \varepsilon^{-1}$ law (see text). In the inset T_1^{-1} is given for $230 < T < 300$ K in an enlarged logarithmic scale.

and final positions remain ideally equivalent sites. Such a decoupling between the two interactions allows to examine separately the low temperature "flutter" motion and the high temperature rotation. It can be quite simple to describe within a Bloembergen-Purcell-Pound model with a temperature activated correlation time, the ^{11}B T_1 anomaly at 250 K (and compare it with ^{19}F data). In the following, the less trivial low temperature behaviour is analysed in terms of an order-disorder transition involving the BF_3 configuration. By introducing a local variable $s_i(t)$ which takes the values 1 or 0 according to occupancy or no occupancy of the i site, one can write [10]

$$T_1^{-1} = \sum_{\boldsymbol{q}} A_{\boldsymbol{q}}\, S(\boldsymbol{q}, \nu_L)\,,$$

where

$$S(\boldsymbol{q}, \nu_L) = \int \exp(i\, 2\pi\, \nu_L\, t)\, \langle s_{\boldsymbol{q}}(0) \cdot s_{-\boldsymbol{q}}(t) \rangle\, \mathrm{d}t$$

is the Fourier transform of the correlation function for the collective critical variable

$$s_{\boldsymbol{q}}(t) = \frac{1}{\sqrt{N}} \sum_n s_n(t) \exp(i\, \boldsymbol{q} \cdot \boldsymbol{r}_n)\,.$$

By assuming, for $T \to T_c$, $A_{\boldsymbol{q}} \approx A_{\boldsymbol{q}_c}$, where $\boldsymbol{q}_c$ is the critical wave vector, and for $S(\boldsymbol{q}, \nu_L)$ the scaling form [10]

$$S(\boldsymbol{q}, \nu_L) = \varkappa^{-2+\eta} \cdot f(q/k)\, \frac{2\pi}{\Gamma_q}\, f'(\nu_L/\Gamma_q)$$

($\varkappa$ = inverse correlation length)

one can write:

$$T_1^{-1} \propto \varepsilon^{-\gamma+\nu(d-z)}\,,$$

where ε is the reduced temperature $[\varepsilon = (T - T_c)/T_c]$, γ, ν, z are critical exponents and d is the lattice dimensionality.

In the mean-field approximation, $\gamma = 1$, $z = 2$, $\nu = 1/2$, and by assuming $d = 3$, one obtains $T_1^{-1} \propto \varepsilon^{-1/2}$, whereas, for $d = 2$, $T_1^{-1} \propto \varepsilon^{-1}$. For $230\ \mathrm{K} > T > T_c$, the experimental data can be roughly fitted by a $T_1^{-1} \propto \varepsilon^{-n}$ law with $n = 1$, in satisfactory agreement with the mean field picture of a two-dimensional correlation as shown in Figure 6.

Conclusions

The dynamics of $(CH_3)_4NBF_4$ has been investigated with different techniques. For $T > T_c = 142$ the motion of the $(CH_3)_4N^+$ ion as a whole appears to be thermally activated with an activation energy $E_a = 5.6$ kcal mol^{-1} and a frequency factor $\tau_0^{-1} = 5.5 \times 10^{13}$ sec^{-1}. Over the whole temperature range investigated, this motion is faster than the rotation of a single CH_3 group.

The definition of the BF_4^- motion is more complicated. From X-ray diffraction, it was established that the boron atom and one of the fluorine atoms lie on a tetragonal axis, whereas the remaining three F^- ions can rotate around it and can occupy eight different positions. For $T = T_c$, a phase transition is observed: the change in the crystal structure gives rise to a jump in the relaxation rate of protons, with a dramatic change in the shape and second moment of the NMR line. The ^{11}B relaxation rate shows an increase of

almost two orders of magnitude, according to a law which does not seem to agree with a mean-field 3 D model. The implications of this fact, possibly in terms of a 2 D model, have to be investigated. The transition is characterized by a volume change, and the transition enthalpy was roughly estimated to be 0.5 ± 0.1 kJ mol^{-1}.

The dynamics of $(CH_3)_4NBF_4$ seems to be fairly similar to that of tetrabutylammonium tetrafluoroborate reported by Szafranska et al. [11]. According to these authors, in the latter salt two phase transitions occur at 270 and 333 K. Experimental evidence for the transition at 333 K was previously found by means of DSC [1] and is confirmed in [11] by a discontinuity in the temperature dependence of the relaxation rate, analogous to that found in the present work.

X-ray diffraction below the transition temperature, adiabatic calorimetry and ^{19}F relaxation rate measurements are now in progress in order to clarify the nature of the phase transition.

Acknowledgements

The authors are grateful to Prof. J. Ziolo for providing some NMR data. The financial support of a 60% MURST Fund is also acknowledged.

[1] G. Zabinska, P. Ferloni, and M. Sanesi, Thermochim. Acta **122,** 87 (1987).
[2] S. Jurga, J. Depireux, and Z. Pajak, Magn. Reson. Relat. Phenom., Proc. Congr. Ampere, 18th, **2,** 403 (1975).
[3] S. Torre and P. Ferloni, Proceedings of the XI IUPAC Conference on Chemical Thermodynamics, Como, Italy, 1990, p. 384.
[4] G. Giuseppetti, F. Mazzi, C. Tadini, P. Ferloni, and S. Torre, Z. Kristallog., in press (1992).
[5] D. J. J. Van Rensburg and J. C. A. Boeyens, J. Solid State Chem. **5,** 79 (1972).
[6] V. Hovi, Proc. Int. Conf. Sci. Technol. of Nonmetallic Crystals, New Delhi, India 1969, p. 67.
[7] S. Albert, H. S. Gutowsky, and J. A. Ripmeester, J. Chem. Phys. **56,** 3672 (1972).
[8] A. Abragam, The Principles of Nuclear Magnetism, Oxford, University Press 1961.
[9] V. H. Schmidt, Pulse response in the presence of quadrupolar splitting, in: Pulsed Magnetic and Optical Resonance, Proceedings of the Ampere International Summer School 2nd, Basko Polje, 2–13 September 1971, edited by R. Blinc, University of Ljubljana, Ljubljana, Yugoslavia, 1972, pp. 75–83.
[10] A. Rigamonti, NMR-NQR studies of structural phase transitions, Adv. Phys. **33,** 115 (1984).
[11] B. Szafranska, Z. Pajak, and A. Kozak, Z. Naturforsch. **46a,** 545 (1991).